J Polym Environ (2013) 21:658–674
DOI 10.1007/s10924-013-0584-0

ORIGINAL PAPER

A Composting Study of Membrane-Like Polyvinyl Alcohol Based Resins and Nanocomposites

Kaiyan Qiu · Anil N. Netravali

Published online: 7 June 2013

Abstract This study presents the effect of biodegradation, in a composting medium, on properties of membrane-like crosslinked and noncrosslinked polyvinyl alcohol (PVA) and nanocomposites. The composting was carried out for 120 days and the biodegradation of these materials was characterized using various techniques. The changes in the PVA resin and nanocomposite surface topography and microstructure during composting were also characterized. The results from the analyses suggest biodegradation of PVA based materials in compost medium was mainly by enzymes secreted by fungi. The results also indicate that the enzymes degraded the amorphous regions of the specimens first and that the PVA crystallinity played an important role in its biodegradation. The surface roughness of the specimens was seen to increase with composting time as the microbial colonies grew which in turn facilitated further microorganism growth. All specimens broke into small pieces between 90 and 120 days of composting as a result of deep biodegradation. Glyoxal and malonic acid crosslinking decreased the PVA biodegradation rate slightly. Addition of highly crystalline microfibrillated cellulose and naturally occurring halloysite nanotubes in PVA based nanocomposites also decreased the biodegradation rate. The three factors: PVA crystallinity, crosslinking and additives, may be utilized effectively to extend the life of these materials in real life applications.

Keywords Polyvinyl alcohol · Crosslinking · Nanocomposites · Biodegradation · Composting

K. Qiu · A. N. Netravali (✉)
Fiber Science Program, Cornell University, Ithaca, NY 14853-4401, USA
e-mail: ann2@cornell.edu

Introduction

Most commercially available polymers and fiber reinforced plastics (composites) at present are non-biodegradable. Also, they are made using petroleum, a non-renewable resource. With double digit increase in the use of plastics and composites in every part of our life, their waste disposal has become a serious problem [1–9]. One of the best ways to address these issues is to use biobased and biodegradable polymers and their composites. As a result, significant effort is being put in developing biobased and biodegradable polymers and composites [1–9]. The research in this field has accelerated in recent years because of the environmental awareness among people as well as the governmental regulations and support [1–9]. Most biobased polymers derived from renewable raw materials, such as cellulose, proteins and carbohydrates (starches) are inherently biodegradable [8]. However, the term 'biodegradable polymers' refers to petroleum-based synthetic polymers, such as polyvinyl alcohol (PVA) which decompose in natural aerobic (composting) and anaerobic (landfill) environments [8–11].

Biodegradation is regarded as a process in which the degradation results from the action of microorganisms such as bacteria, fungi or algae [12, 13]. Biodegradation can be divided into two steps [13]. In the first step 'depolymerization' the polymer chain undergoes backbone scission and fractures into smaller oligomeric fragments, facilitated by the enzymes secreted by microorganisms. In the second step 'mineralization' small oligomeric fragments are converted to biomass, minerals and salts, water and gaseous substances such as carbon dioxide and methane by microorganisms [13]. While the biodegradation process is chemical in nature, the attacking chemicals (enzymes) come from microorganisms [14–18]. Biodegradation

results in the changes in surface properties as the microorganisms begin their attack at the surface. Once progressed, it results in severe degradation through breakage of backbone chains that lowers polymer molecular weight as well as the mechanical and thermal properties [12–21].

The microorganism based biodegradation for many polymers and composites has been extensively studied [1–3, 8, 12, 22–34]. Many factors have been shown to influence the biodegradation process and include, among others, surface area, hydrophilic/hydrophobic nature, chemical structure, molecular weight, crystallinity, crosslinking and melting temperature.

PVA is a widely used thermoplastic and biocompatible polymer. Its crosslinked products and nanocomposites with nanofillers also have been widely investigated [4, 6, 7]. However, unlike most petroleum based polymers, it is one of the rare polymers with carbon–carbon single bond backbone that is fully biodegradable in the presence of suitably acclimated microorganisms [1, 2, 8]. In addition, because of the hydroxyl (–OH) groups on alternating carbon atoms, PVA is hydrophilic and water soluble, which also promotes its degradation through hydrolysis [1, 2, 8, 9, 35, 36]. The first microorganisms capable of assimilating PVA as their sole carbon source were isolated from soil samples and identified as *Pseudomonas* species [2, 9, 28, 29, 36, 37]. Further studies confirmed that other aerobic bacteria, such as *Alcaligenes* and *Bacillus*, can also degrade PVA [9, 27, 37–39]. Fungal strains, such as *Aspergillus niger*, *Pycnoporus cinnabarinus*, *Fusarium* and *Phanerochaete chrysoporium*, have also been reported to change the polymer (like PVA) surface from smooth to rough and to break down the polymer [9, 40, 41]. In these studies, while it was assumed that the initial microbial attack was consistent with the polymer chain cleavage, occurrence of oxidative reactions of the tertiary carbon atoms of PVA chains, leading to the formation of hydrolysable β-hydroxylketone and 1, 3-diketone groups along the polymer backbone, was also established. These reactions were catalyzed by specific oxidases and dehydrogenases that were isolated mainly as extracellular proteins from different bacterial species [1, 2, 9, 27]. However, biodegradation of PVA cannot be finished by a single kind of microorganism in a natural biodegradative environment, instead, it is the combinative process accomplished by many microorganisms working simultaneously [37–41].

Many polymers including PVA have been shown to degrade under different environmental conditions, including aerobic composting, soil burial, aqueous media and even anaerobic conditions [27, 42–45]. Among these methods, composting is an effective way to characterize the biodegradation of PVA and other polymers and their composites [2]. Composting is defined as an exothermic bio-oxidative decomposition of organic materials by indigenous microorganisms in a controlled moist and warm aerobic environment leading to the production of 'compost', a mixture of carbon dioxide, water, minerals and a stabilized organic matter [28, 46]. As the compost becomes active, mesophilic and thermophilic microorganisms secrete depolymerase enzymes that attack the substrate as nutrient [28, 46]. Biodegradability, in compost environment, of PVA/starch blends and their crosslinked products have been investigated and found to be fully biodegradable [47, 48]. Their results indicated PVA with higher molecular weight has higher biodegradability and crosslinking retarded the biodegradation during the initial part of composting [47, 48].

The present study was conducted to understand the effect of crosslinking and additives on the biodegradation of PVA and its nanocomposites. Typical composting technique was utilized to characterize the biodegradation of PVA based materials, including PVA, glyoxal crosslinked PVA (GX-PVA), malonic acid crosslinked PVA (MX-PVA), microfibrillated cellulose (MFC)-PVA nanocomposite and halloysite nanotube (HNT)-PVA nanocomposite. Various characterization methods were used to understand the biodegradation process. Weight loss was monitored as a function of biodegradation. The results indicate that it is possible to control the biodegradation through PVA morphology (crystallinity), crosslinking and additives and, thus, extend the useful life of these materials in real applications.

Materials and Methods

Materials

PVA powder (M_w 31,000–50,000, 98–99 % hydrolyzed), glyoxal solution (25 wt% solution), malonic acid (MA) powder and Tween® 80 (non-ionic surfactant) were purchased from Sigma-Aldrich, St. Louis, MO. Phosphoric acid (85 wt% solution in water) was purchased from Mallinckrodt Baker, Phillipsburg, NJ. MFC in water (KY-100G) was obtained from Daicel Chemical Industries, Japan. Halloysite nanotubes (HNTs) in raw form were obtained from Nanoclays and Technology Inc, Utah (Division of Atlas Mining). Composting chicken manure was obtained from Poultry Research Farm, Cornell University, Ithaca, NY. Sawdust (Fine Pine Shavings) was purchased from Tractor Supply Co., Ithaca, NY, USA.

Specimen Preparation

Preparation of PVA, GX-PVA and MX-PVA

PVA powder was added to deionized water at weight ratio of 1:9 to form PVA solution kept in a water bath at 80 °C

and stirred for 30 min. Glyoxal solution and MA powder were then added separately, to PVA solutions. The glyoxal:PVA weight ratio was 3:100 and MA:PVA weight ratio was 10:100 [6, 7]. The pH of both mixtures was adjusted to 1 using phosphoric acid. Both mixtures were stirred at 90 °C for 1 h to precure. The precured mixtures were then cast on Teflon® coated glass plates and slowly dried in an air circulating oven at 40 °C to form precured crosslinked PVA sheets. The precured crosslinked PVA sheets were hot pressed in a Carver hot press (model 3891) at 100 °C at a pressure of 0.2 MPa for 60 min to form crosslinked PVA sheets. Acetal linkage are formed between hydroxyl groups of PVA and carbonyl groups of glyoxal during the hot pressing, while ester linkages are formed between hydroxyl group of PVA and carboxylic groups of MA [6, 7, 49, 50]. The MA crosslinked PVA specimens were immersed in deionized water at RT for 12 h to remove the phosphoric acid used as catalyst and the unreacted MA. Cured GX-PVA sheets were not treated by water in order to observe the effect of the residual catalyst (phosphoric acid) on the composting behavior. The specimens were then dried at 40 °C in an air circulating oven to form final GX-PVA and MX-PVA sheets. Control PVA sheet specimens were prepared by casting PVA solution without the addition of glyoxal or MA, for comparison. Average thicknesses of the sheets were approximately 0.2 mm in all cases.

Preparation of MFC-PVA and HNT-PVA Nanocomposites

MFC in water and HNT powder were prepared as MFC suspension and individualized HNT dispersion, respectively, for fabrication of nanocomposites [6, 7]. Briefly, the MFC was added to deionized water at the weight ratio of 1:199 and stirred using high speed at 90 °C and 1,000 rpm for 1 h and followed by ultrasonication (Branson Ultrasonics, Model 2510, Mumbai, India) at 65 °C for 1 h in order to individualize the fibrils and form MFC suspension (0.5 % MFC by wt). The fibrils have broad range of diameters from a micrometer to a couple of hundred nm as well as a broad distribution of lengths [6, 51]. HNT powder was initially added to deionized water at a weight ratio of 1:49. Tween® 80 (HNT:Tween® 80 (w/w) = 10:1) was then added to the mixture, as non-ionic surfactant, to assist in individualizing the HNTs. The pH value of the mixture was adjusted to 10 using NaOH solution, to further avoid clustering of HNTs [52]. The mixture was stirred at 90 °C and 1,000 rpm for 1 h followed by ultrasonication at 65 °C for 1 h to form original HNT dispersion. The original HNT dispersion was kept standing for 2 days to stabilize. The supernatant of the HNT dispersion was used as the final individualized HNT dispersion. The HNT loading in the final individualized HNT dispersion was 0.5 % by wt. The PVA solution (10 % by wt) was added to either the MFC suspension or the final individualized HNT dispersion, in desired weight ratios. The MFC-PVA solution and HNT-PVA solutions were stirred at 90 °C for 1 h and ultrasonicated at 65 °C for 1 h. Both mixtures were cast on Teflon® coated glass plates and slowly dried in an air circulating oven at 40 °C to form MFC-PVA (10 % MFC content, by wt) and HNT-PVA nanocomposite sheets (10 HNT loading, by wt, in the nanocomposites). The MFC-PVA and HNT-PVA nanocomposites were hot pressed at 100 °C and 0.2 MPa for 60 min to form the final nanocomposites with smooth surfaces and thicknesses of about 0.2 mm.

Composting Set-up

The composting medium was prepared by blending chicken manure (droppings) and sawdust in the ratio 1:1 (w/w) to obtain a C/N ratio of 50/50 [1–3, 28].

All specimens were dried in an oven at 105 °C for 12 h and then placed in porous non-woven polypropylene (NPP) bags, which were then placed in the compost mix for microbial degradation. The NPP bags facilitated easy retrieval of the buried sheet specimens and its open structure allowed moisture, air and microorganism to move in and out freely during composting. The composting conditions such as moisture, temperature, pH were monitored periodically. The moisture content of the compost mix was maintained at 50 % by adding water initially and periodically. The temperature of the compost mix was maintained at 32 °C (in mesophilic phase) throughout the composting. This assured that the degradation was primarily attributed to the activity of mesophilic microorganisms, actinomycetes and fungi. The pH of the compost was measured to be acidic in the range of 5.5–6.0 during composting. There is no evidence that the PVA based specimens or products can degrade themselves in this pH range. In addition, PVA solution has a low degradation rate close to this pH range by hydrolysis under ultrasonic environment [36]. Composted specimens were retrieved after 30, 45, 60, 75, 90 and 120 days of composting. The specimens were dried in an oven at 105 °C for 12 h again and characterized for various properties [1–3, 28].

Characterization

Surface Characterization During Composting

The non-composted (control) and composted PVA, GX-PVA, MX-PVA and MFC-PVA and HNT-PVA nanocomposite specimens were sputter coated with gold prior to scanning electron microscopy, SEM, (Leica 440, Leica Microsystems, Cambridge, UK) at a voltage of 15 kV.

Weight Loss

All control and composted specimens were dried in an air circulating oven at 105 °C for 12 h and weighed. The percent weight (wt) loss was calculated using the ratio of lost wt to original wt.

Attenuated Total Reflectance-Fourier Transform Infrared (ATR-FTIR) Spectroscopy

Chemical analysis of the dried specimen surfaces was carried out using an FTIR spectrophotometer (Nicolet Magna-IR 560, Thermo Scientific, Waltham, MA, USA) in attenuated total reflection (ATR) mode using split pea accessory. Spectra, averaged over 64 scans, were taken in the range of 4,000–800 cm^{-1} wavenumber at a resolution of 4 cm^{-1}.

Differential Scanning Calorimetry

Differential scanning calorimetry (DSC, Model Q2000, TA Instruments Inc., New Castle, DE, USA) was used to analyze the glass transition temperature (T_g), melting temperature (T_m), enthalpy of fusion (ΔH_f) and crystallinity of the specimens. All specimens were dried as mentioned above prior to conducting the test. All DSC tests were performed under a nitrogen atmosphere by keeping the flow rate of 50 ml/min, between −20 and 250 °C and at a scanning rate of 10 °C/min.

Sol–Gel Analysis of the Resins

PVA, GX-PVA and MX-PVA specimens were taken out after specific composting periods and dried prior to conducting the sol–gel test. The specimens were weighed to obtain their initial dry wt and then immersed in distilled water in 150 mL glass bottles. The glass bottles with the specimens were placed on a shaker table (MAXQ 4450, Thermo Scientific, Waltham, MA, USA) maintained at 80 °C and 150 rpm for about 2 h or until the control (noncrosslinked) PVA was completely dissolved. The remaining solids content for the crosslinked specimens were then washed three times with distilled water and filtered using a Whatman® filter paper (Number 4, 20–25 μm pore size) to obtain final residues. The water soluble part (sol) and particles smaller than 25 μm were removed during filtration. The final residues of the GX-PVA and MX-PVA specimens were fully dried to obtain their dry wt (gel). Ratios of the gel wt of the crosslinked PVA to their corresponding initial dry wt were used as PVA gel (crosslinked) percentages.

Energy Dispersive X-Ray Analysis

The elemental composition of crystals observed on the surface of GX-PVA and MX-PVA specimens were analyzed by energy dispersive X-ray technique (EDX, Bruker AXS Microanalysis GmbH Berlin, Germany) with primary energy of 9 keV with 90-s scans.

Results and Discussion

Surface Characterization (SEM and EDX) During Degradation

Typical SEM photomicrographs showing surface characteristics of PVA (control), GX-PVA, MX-PVA and MFC-PVA (10 wt% MFC content) and HNT-PVA nanocomposites (10 wt% HNTs loading) as a function of composting days are presented in Figs. 1, 2, 3, 4 and 5, respectively.

As can be seen in Fig. 1a, the control PVA specimens showed a relatively smooth surface before composting. After 30 days of composting no significant difference was observed on its surface topography (Fig. 1b). However, some traces were obvious on the surface of the resin after 45 days of composting (Fig. 1c). These traces, branched filamentous structures, are known as fungal hyphae [53, 54]. In most fungi, hyphae are the main mode of vegetative growth. In the present case these were generated since the composting temperature was maintained in the mesophilic phase and confirm the findings of the earlier studies [53, 54]. The number of fungal hyphae on the resin increased after 60 and 75 days of composting shown in (Fig. 1d) and (Fig. 1e), respectively, with some crisscrossing each other. Some grooves along with more fungal hyphae were observed on the surfaces of PVA specimens after 90 days of composting indicating deeper biodegradation of the specimens (Fig. 1f). Fungal hyphae and deeper cracks spread everywhere on the surface of PVA specimen that resulted in specimens breaking down into many small pieces after 120 days of composting (Fig. 1g). Similar results were observed earlier for poly(3-hydroxybutyrate-co-3-hydroxyvalerate) (PHBV) during its biodegradation [52].

In the case of crosslinked GX-PVA specimens, a different sequence of biodegradation was observed. As seen in Fig. 2a, the control GX-PVA specimens showed smooth surface before composting. After 30 days of composting, surface of the resin began to get rougher and showed a layer with crystal-like elements (Fig. 2b). These crystals were assumed to be formed by the residual catalyst phosphoric acid that had leached out and crystalized on the surface during composting [55]. The presence of residual phosphoric acid and possibly its salts on the surface of the specimen were confirmed using energy-dispersive X-ray

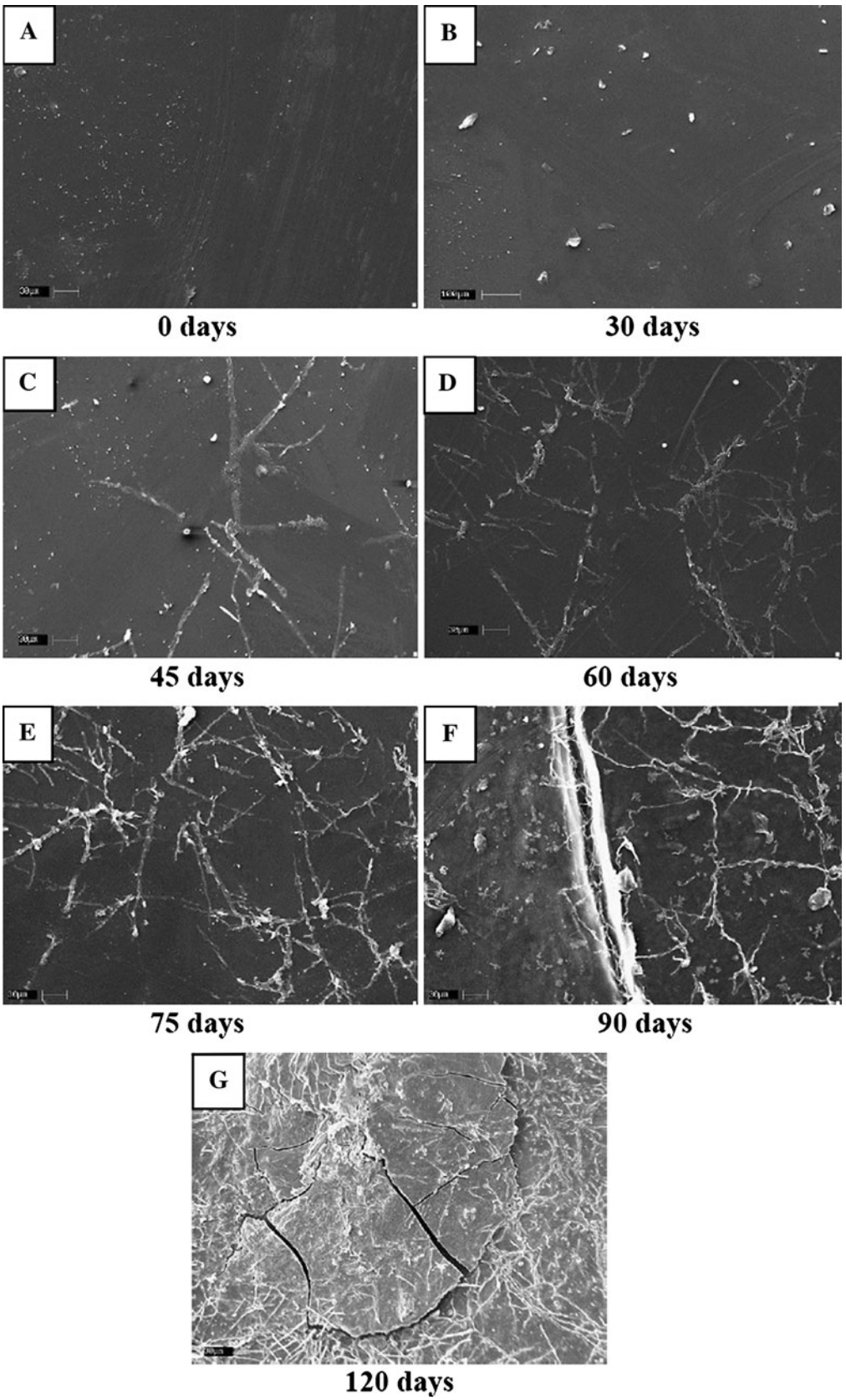

Fig. 1 SEM photomicrographs showing the surface characteristics of PVA specimens as a function of composting time

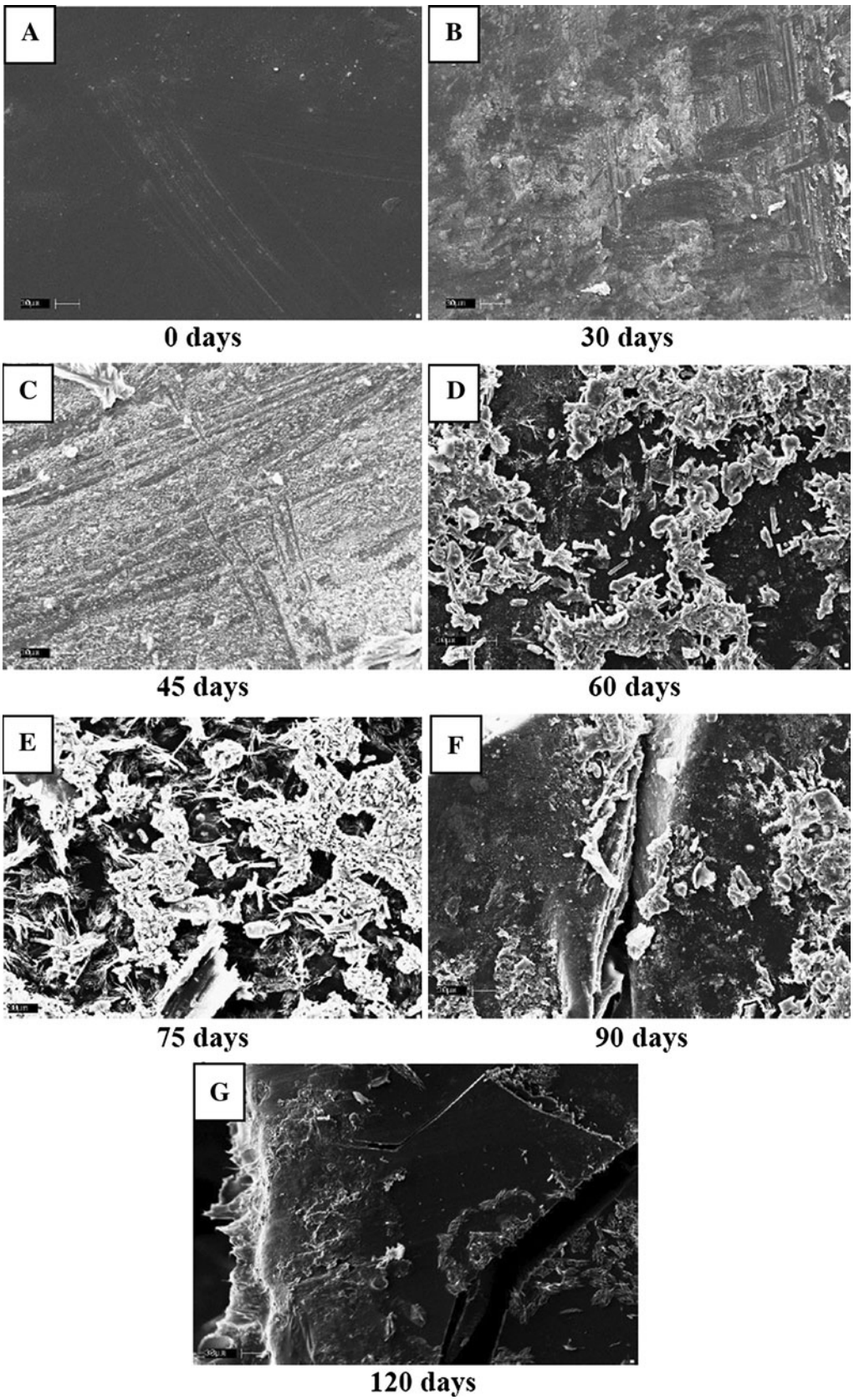

Fig. 2 SEM photomicrographs showing the surface characteristics of GX-PVA specimens as a function of composting time

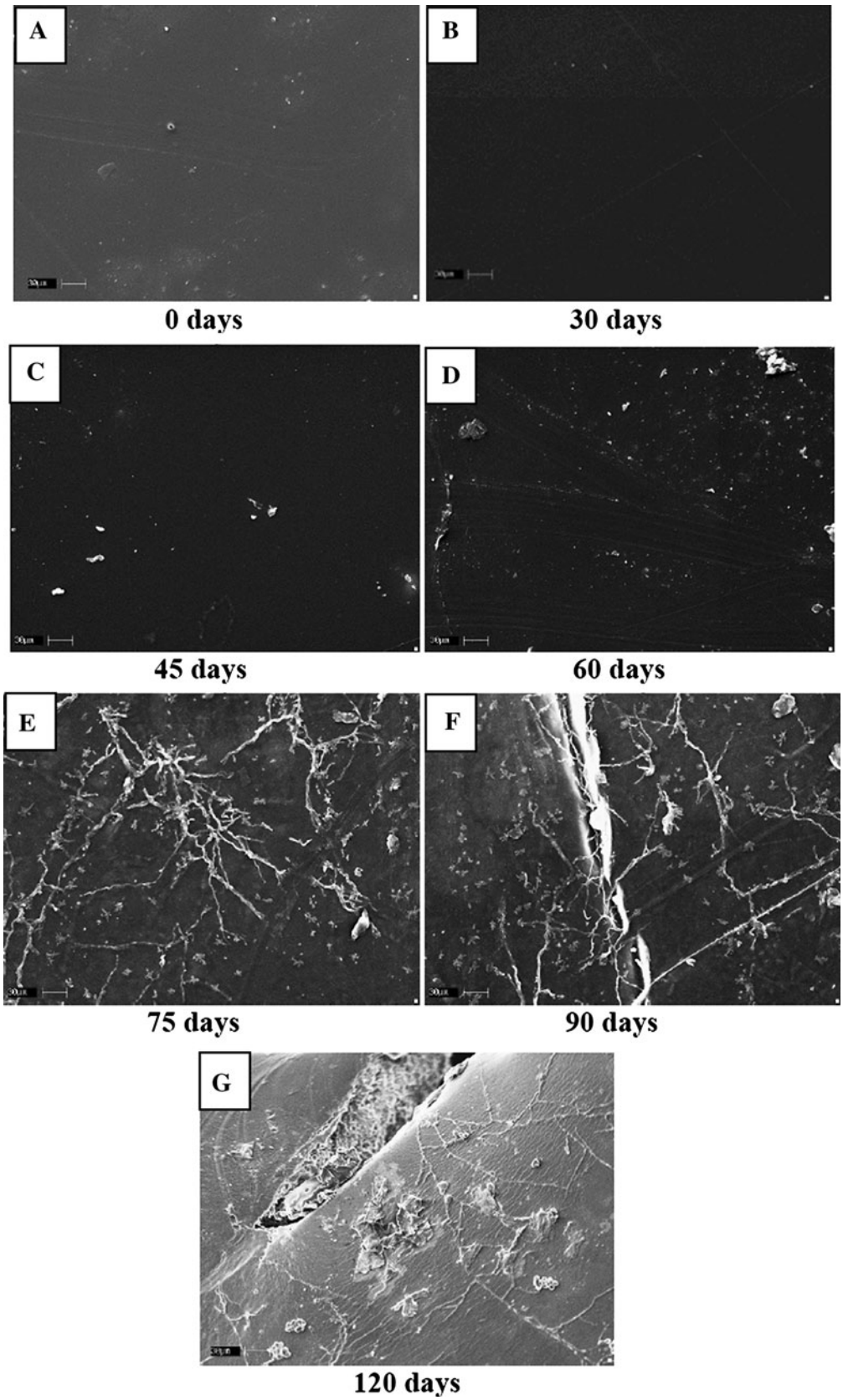

Fig. 3 SEM photomicrographs showing the surface characteristics of MX-PVA specimens as a function of composting time

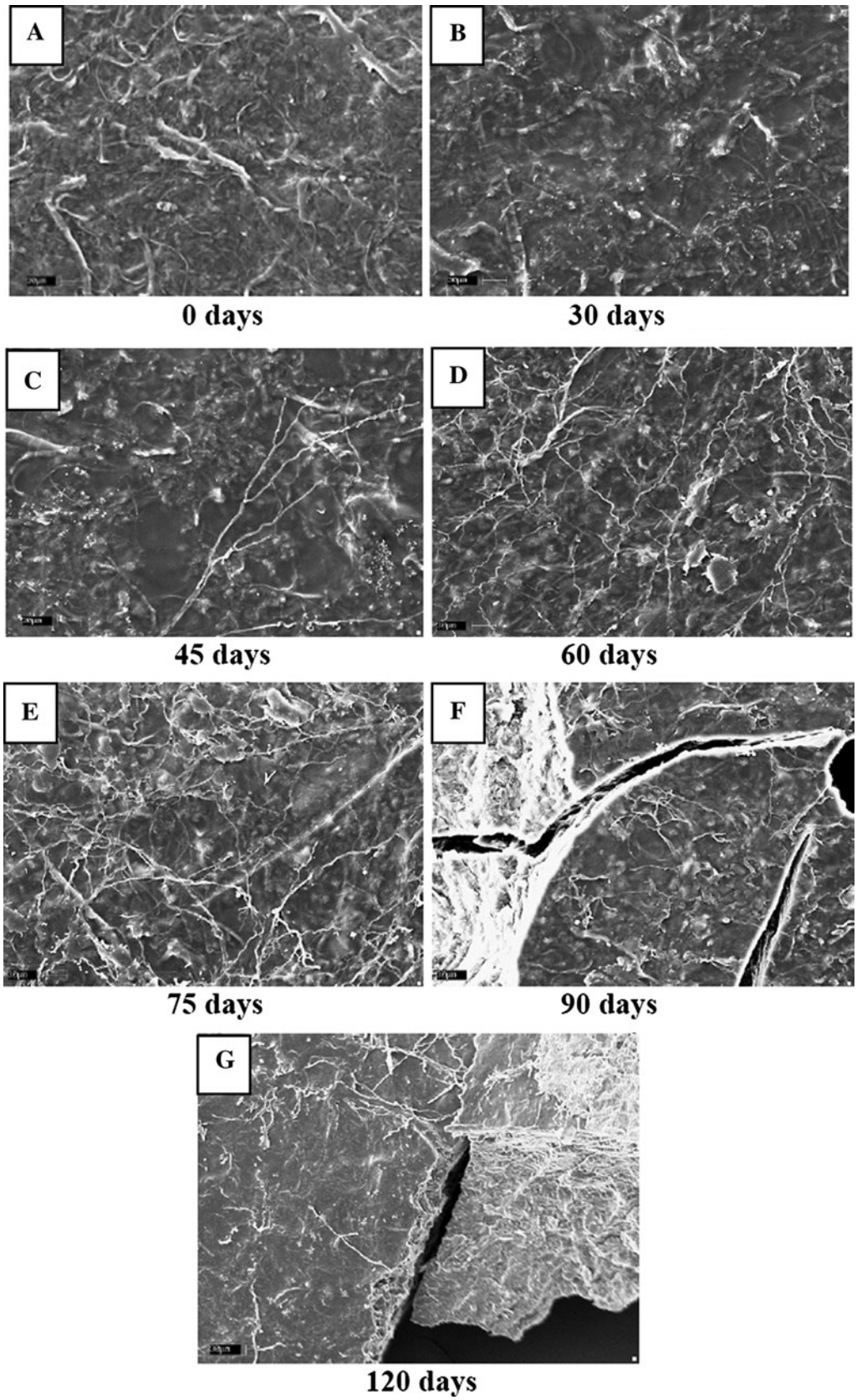

Fig. 4 SEM photomicrographs showing the surface characteristics of MFC-PVA nanocomposites (10 wt% MFC content) as a function of composting time

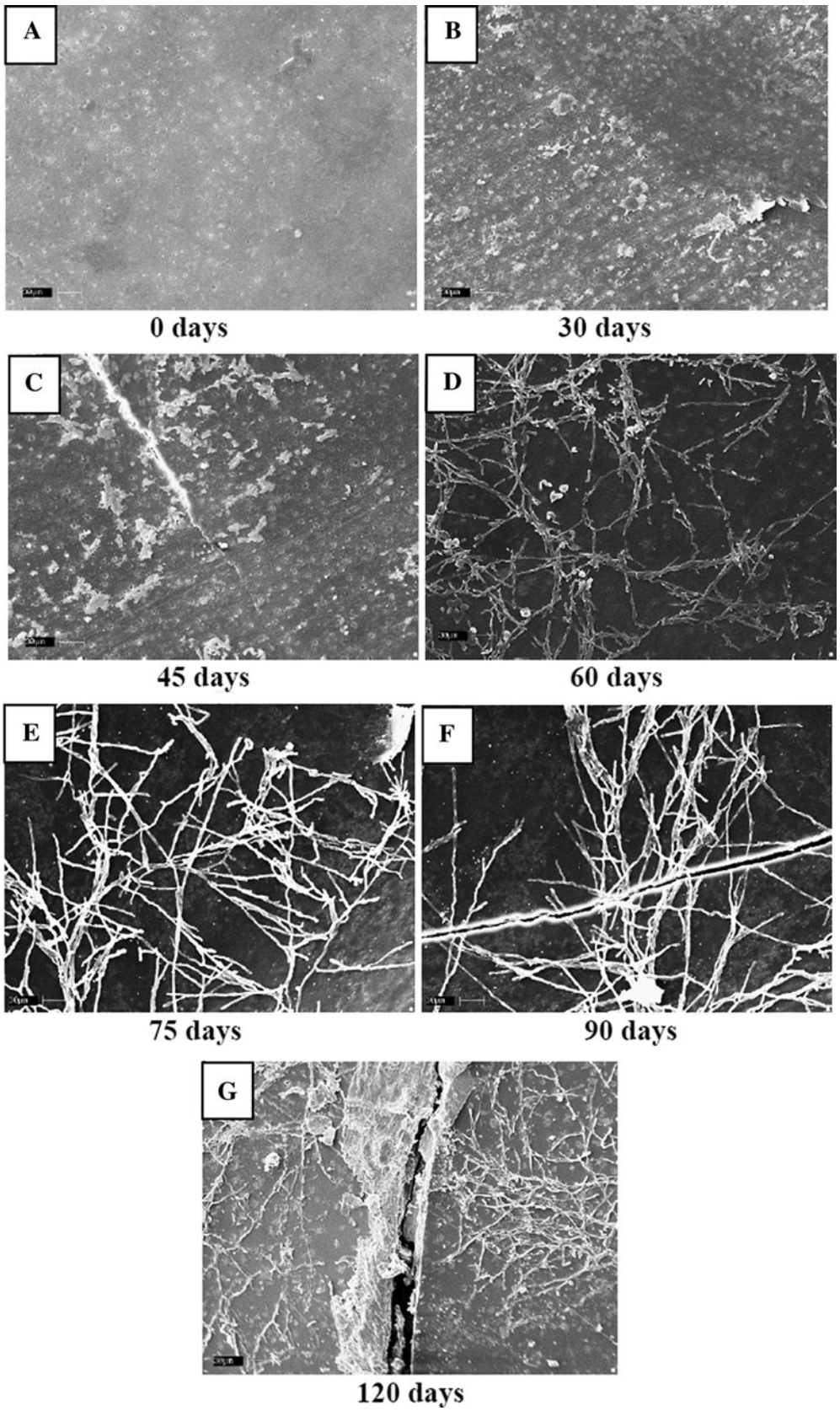

Fig. 5 SEM photomicrographs showing the surface characteristics of HNT-PVA nanocomposites (10 wt% HNTs loading) as a function of composting time

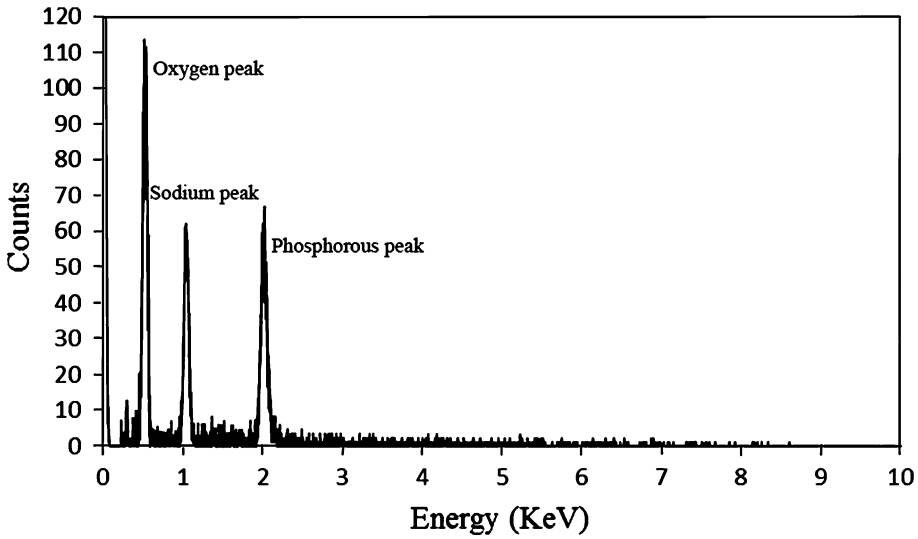

Fig. 6 EDX spectrum showing elements in crystals on the surface of GX-PVA and MX-PVA specimens after composting

(EDX) analysis. A typical EDX spectrum showing a strong peak for phosphorous at 2 keV (Energy axis) is presented in Fig. 6. Other two strong peaks seen in Fig. 6 are for oxygen at 0.5 keV and sodium at 1.1 keV respectively. The sodium peak is very likely from sodium salts present in the chicken manure [56]. After 45 days of composting, the surface roughness of the resin increased and the thickness of the crystal layer increased as well (Fig. 2c). This is mainly because more residual catalyst phosphoric acid leaches out and forms salts during the compost process. However, the size of crystals remained constant. The crystalline structure of the layer became even more obvious on the surface of the resin after 60 days of composting (Fig. 2d). The crystal layer spread all over the surface of the specimen along with some grooves after 75 days of composting (Fig. 2e). After 90 days, deeper grooves were seen indicating significant biodegradation of GX-PVA (Fig. 2f). While the specimen broke down into many small pieces at the end of 120 days of composting, deep cracks were seen on their surfaces (Fig. 2g). Fungal hyphae were not seen on GX-PVA surfaces during composting. However, it is possible that they were covered by the thick crystalline phosphoric acid or salt layer.

The crosslinked control MX-PVA specimens also showed smooth surfaces as seen in Fig. 3a. After 30 and 45 days of composting, no obvious changes except some small crystals were observed on their surfaces (Fig. 3b, c). These crystals, as mentioned earlier, resulted from leached residual phosphoric acid and its salts as confirmed by EDX [55]. After 60 days, more crystals were seen on the specimen surfaces (Fig. 3d). However, the amount of residual phosphoric acid was less on the surface of MX-PVA than on the surface of GX-PVA. This is because less phosphoric acid was needed for preparing MX-PVA specimens since MA also helped lowering the pH to 1 used for crosslinking. Another reason is that the MA crosslinked specimens were treated by water to partially remove some phosphoric acid after crosslinking. After 75 days of composting, many fungal hyphae appeared on the specimen surfaces (Fig. 3e) and after 90 days a few grooves were seen along with more fungal hyphae (Fig. 3f). Deep cracks were also seen on the surface and the specimen broke into small pieces after 120 days of composting suggesting high extent of biodegradation of MX-PVA (Fig. 3g).

It can be clearly seen from Fig. 4a that the MFC fibrils are randomly organized but uniformly distributed on the MFC-PVA nanocomposite specimen surface. It is assumed that the MFC fibrils are uniformly distributed within the MFC-PVA nanocomposite as well. After 30 days of composting, no significant difference can be seen in the nanocomposite surface (Fig. 4b). However, some fungal hyphae were observed on the surface of the nanocomposite after 45 days (Fig. 4c). The number of fungal hyphae increased after 60 days of composting (Fig. 4d) and some finer grooves appeared on the surfaces after 75 days (Fig. 4e). After 90 days of composting, the grooves became larger and deeper resulting in the specimen breaking into smaller fragments (Fig. 4f). The specimens composted for 120 days showed deeper cracks and again broke into many smaller pieces (Fig. 4g).

The control HNT-PVA nanocomposites (Fig. 5a) also had smooth surfaces. After 30 days of composting, no obvious change was observed on their surfaces (Fig. 5b) and only a few spots and even cracks were seen after 45 days of composting (Fig. 5c). Fungal hyphae were observed only after 60 days of composting (Fig. 5d) which increased significantly and were seen randomly distributed on the surfaces after 75 days of composting (Fig. 5e). After 90 days deeper grooves were seen which lead the specimen breaking up (Fig. 5f). Deeper cracks appeared after

120 days of composting the specimens were seen to break into pieces (Fig. 5g).

In summary, the SEM results indicated that the fungi played an important role during biodegradation of the PVA based materials. The fungal hyphae were seen to spread over the surface of all PVA based specimens and initiating the degradation during composting [40, 41]. With additional composting time, surface roughness of specimens increased, especially after 75 days. While the roughness is an important factor that facilitates the specimens breaking into pieces, it also expedites the biodegradation rate by providing additional surface for the fungi to attack. Crosslinking (GX and MX) and filler addition (MFC and HNT), to some extent, decreased the biodegradation rate of the PVA materials.

Weight Loss During Composting

The effect of composting time on the weight loss of the PVA, GX-PVA, MX-PVA and MFC-PVA and HNT-PVA nanocomposite specimens is presented in Fig. 7. The data in Fig. 7 indicate, the weight loss for PVA specimen is 0.2, 2.1, 2.7, 3.2, 5.2 and 20.1 % after 30, 45, 60, 75, 90 and 120 days of composting, respectively. While the weight loss was small (0.2 %) during the first 30 days of composting, it accelerated between 90 and 120 days (15 %) and specimens also broke into small pieces. Such rapid weight loss after 90 days of composting confirms the results obtained by other researchers [8]. Crosslinked GX-PVA specimens, however, showed a relatively higher weight loss, 3.2 % in the first 30 days of composting. This was primarily due to the leaching of residual catalyst phosphoric acid in the resin. Once the phosphoric acid was leached out the rate of weight loss of GX-PVA specimens decreased and was slightly lower than control PVA specimens, although the total weight loss was higher. For example, the weight loss between 30 and 45 days of composting was only 0.3 %. After 120 days, the weight loss of GX-PVA specimens only reached to 15.1 %, lower than over 20 % observed for control PVA specimens. The real weight loss, considering about 3 % loss of phosphoric acid, is only about 12 %. This is because glyoxal crosslinking, though only partial, decreased the biodegradation rate. Such reduced degradation rate by different chemical crosslinking for other polymers has been reported earlier [6, 34, 57]. The weight loss for MX-PVA specimens reached 0.8 % after 30 days of composting. While this was higher than that obtained for PVA specimens, it was lower than GX-PVA specimens. This, again, is due to the leaching out of residual catalyst phosphoric acid in the resin. However, much lower amount of phosphoric acid was used in the case of MX-PVA specimens since MA was able to reduce the pH. Once the phosphoric acid leached out, the biodegradation rate of MX-PVA specimens decreased and was lower than both control PVA and GX-PVA specimens. Weight losses for MX-PVA specimens were 0.9, 1.0, 1.1, 2.1 and 10.1 %, after 45, 60, 75, 90 and 120 days of composting, respectively. This lower biodegradation is because MA is a better crosslinking agent compared to glyoxal and results in higher crosslinking [6, 7, 34]. This conclusion was further confirmed by sol–gel results which are described later. For MFC-PVA and HNT-PVA nanocomposites, the initial weight losses were close to those of PVA specimens, about 0.1 % after 30 days of composting. However, the nanocomposites lost lower weight than PVA thereafter. These results contradict with some of the previous reports suggesting that addition of dispersed phase can increase the biodegradation rate of polymers [30–33]. However, in the present case, it is because the MFC is highly crystalline and provides crack-bridging that delays breaking apart of the PVA film. In the case of HNTs they themselves do not degrade and influence the process during composting. From Fig. 7, sharp increase in weight losses can be observed for all specimens from 75 to 120 days of composting confirming the SEM

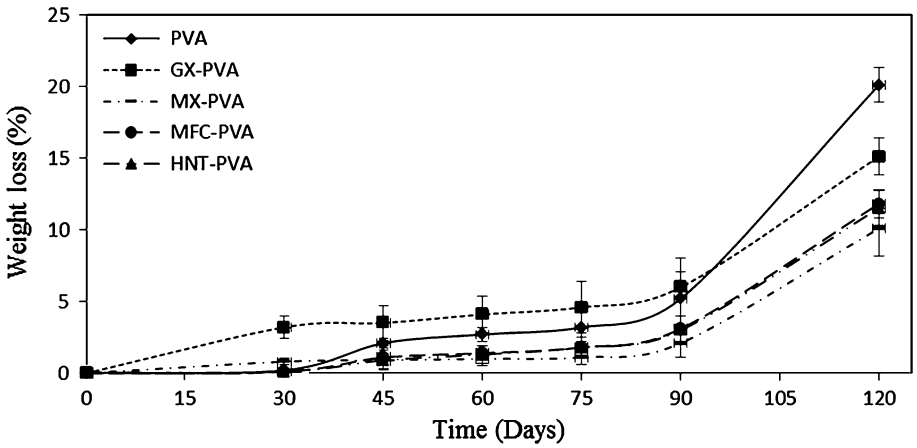

Fig. 7 Effect of composting time on the weight loss (%) of PVA, GX-PVA, MX-PVA, MFC-PVA nanocomposite and HNT-PVA nanocomposite

results of specimen breaking in that period. The increased surface roughness provides additional surface for the fungi to act and, thus, may also expedite the biodegradation.

ATR-FTIR Spectroscopy

The effect of composting time on the PVA specimen surface chemistry analyzed using ATR-FTIR and is presented in Fig. 8, where spectra (a), (b) and (c) represent PVA specimens after 0, 60 and 120 days of composting, respectively. A broad band at 3,500–3,200 cm^{-1} wavenumber seen in all three spectra is a result of the O–H stretching vibration resulting from the intra-molecular and inter-molecular hydrogen bonding in PVA [58–60]. The absorption band observed between 3,000 and 2,820 cm^{-1} wavenumbers is due to the stretching of the aliphatic C–H bonds [58]. The absorbance intensity ratio of O–H to C–H bands showed a decrease from 1.81 in spectrum (a) for control PVA specimen compared to 1.32 for spectrum (b) (60 days of composting) and 1.11 for spectrum (c) (120 days of composting). The lower ratio clearly indicates a reduction in the O–H groups and confirms degradation of PVA with composting time as explained by Chiellini et al. [9]. Absorption at 1,750–1,600 cm^{-1} (stretching of C=O) for PVA before composting (spectrum (a)) was weak (intensity ratio of C=O to C–H = 0.51) and indicates the presence of carbonyl (C=O) in the resin from the nonhydrolyzed acetate group remaining in the PVA, confirming earlier results by Gohil et al. [58] and Mansur et al. [59]. In the ATR-FTIR spectrum (b), however, a slightly sharper absorption (intensity ratio of C=O to C–H = 0.55) observed at 1,750–1,600 cm^{-1} indicates presence of more C=O in the PVA after 60 days of composting. This confirms PVA biodegradation that results in the formation of β-hydroxylketone and 1, 3-diketone groups by a random cleavage of the polymer chains catalyzed by the enzymes [9, 37, 38]. In the ATR-FTIR spectrum (c), a much higher absorption (intensity ratio of C=O to C–H = 1.13) observed at 1,750–1,600 cm^{-1} wavenumber indicates presence of many more C=O groups in PVA after 120 days of composting. This is expected due to continued biodegradation with composting time. These results also indicate formation of ketone groups during composting based on the decreased absorption intensity for O–H stretching vibration combined with the increased intensity of bands for C=O stretching vibrations.

The effect of composting time on GX-PVA specimen surface chemistry by ATR-FTIR is presented in Fig. 9, where spectra (a), (b) and (c) represent GX-PVA after 0, 60 and 120 days of composting, respectively. Two broad bands at 3,500–3,200 cm^{-1} and 3,000–2,820 cm^{-1} wavenumber are due to O–H stretching and aliphatic C–H stretching as mentioned earlier [58–60]. For spectrum (a), the two bands are well separated, and the absorbance intensity ratio of bands for O–H to C–H is 1.28, which is lower than that obtained for pure PVA due to crosslinking of the O–H groups. However, for spectra (b) and (c), no obvious separation was observed between these two bands. This is because of the leaching out of the residual phosphoric acid (catalyst) and crosslinker (glyoxal) during composting. In addition, the absorbance intensity ratio of O–H to C–H bands decreased to 1.11 and 0.87, respectively, for spectra (b) and (c). The lower absorption indicating a reduction in the O–H groups confirms degradation of PVA with composting time. Absorption at 1,750–1,600 cm^{-1} (stretching of C=O) for control GX-PVA (spectrum (a)) was weak (intensity ratio of C=O to C–H = 0.63) and indicates the presence of carbonyl (C=O) in the specimens from residual unreacted aldehyde groups from glyoxal and the nonhydrolyzed acetate groups in

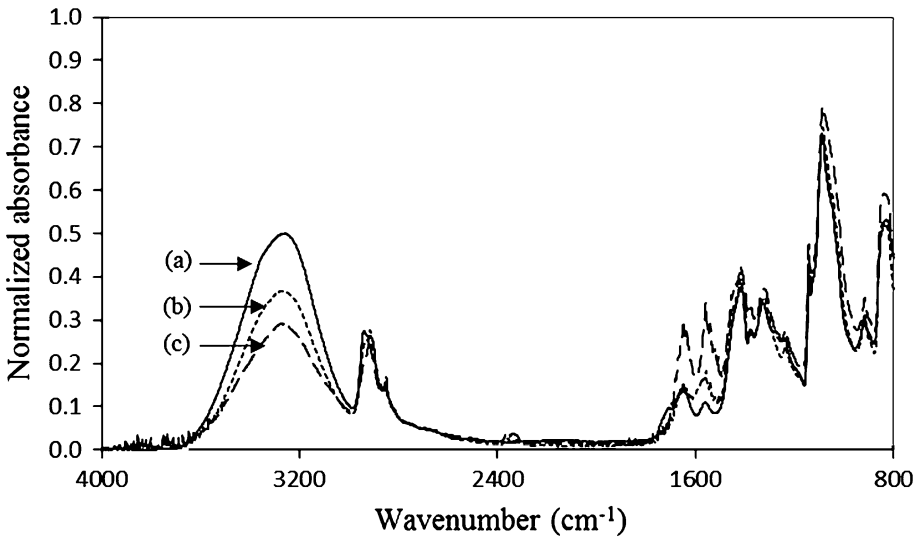

Fig. 8 ATR-FTIR spectra of PVA after 0 days (*a*), 60 days (*b*) and 120 days (*c*) of composting

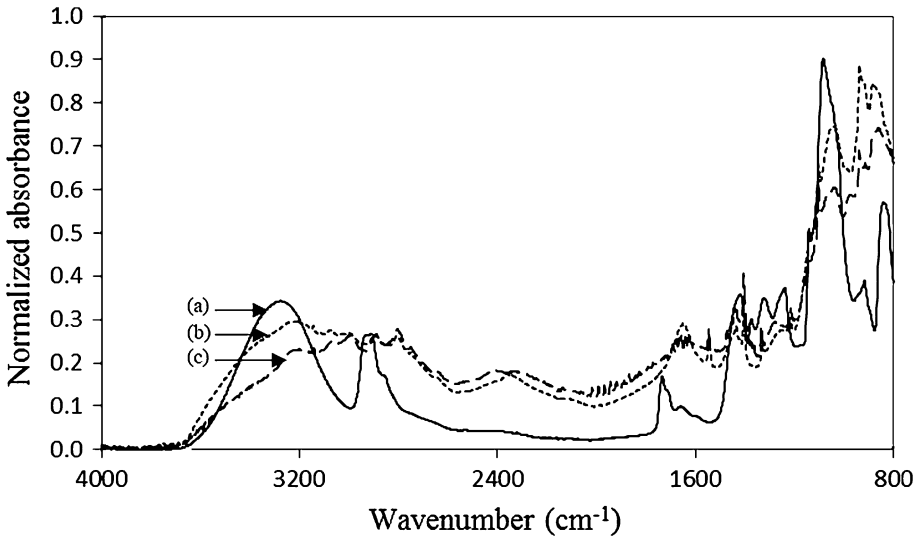

Fig. 9 ATR-FTIR spectra of GX-PVA after 0 days (*a*), 60 days (*b*) and 120 days (*c*) of composting

PVA. In the ATR-FTIR spectra (b), however, a much sharper absorption (intensity ratio of C=O to C–H = 1.09) observed at 1,750–1,600 cm^{-1} wavenumber indicates presence of higher number of C=O groups in the GX-PVA after 60 days composting. This increase in intensity is due to the ketone groups obtained from the biodegradation of GX-PVA [1, 2, 9, 27]. In the ATR-FTIR spectrum (c), the intensity ratio of C=O to C–H observed at 1,750–1,600 cm^{-1} wavenumber is 1.08, almost similar with that in spectrum (b). Glyoxal has been reported as a biodegradable chemical and can degrade during composting [57]. Therefore, more ketone groups generated from degrading GX-PVA helped to maintain the intensity of C=O in spectrum (c).

The effect of composting time on MX-PVA specimen surface chemistry by ATR-FTIR is presented in Fig. 10, where spectra (a), (b) and (c) represent MX-PVA after 0, 60 and 120 days of composting, respectively. As seen in spectra (a), (b) and (c), during composting, the absorbance intensity ratio for O–H to C–H bands showed a decrease from 1.42 in spectrum (a) for control MX-PVA compared to 1.37 for spectrum (b) (60 days of composting) and 1.22 for spectrum (c) (120 days of composting). The lower absorption indicates a reduction in the O–H groups and confirms degradation of MX-PVA at the surface with composting. Absorption at 1,750–1,600 cm^{-1} (stretching of C=O) for MX-PVA before composting (spectrum (a)) was relatively weak (intensity ratio of C=O to C–H = 0.46) and indicates the presence of carbonyl (C=O) in the resin from residual MA and the nonhydrolyzed acetate group in the PVA [58, 59]. In the ATR-FTIR spectrum (b), however, a slightly sharper absorption (intensity ratio of C=O to C–H = 0.50) observed at 1,750–1,600 cm^{-1} indicates presence of higher number of

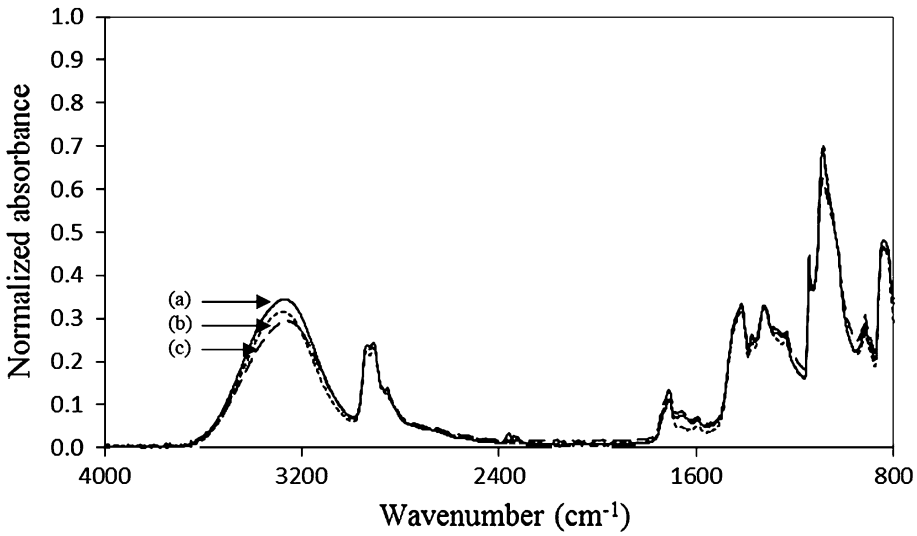

Fig. 10 ATR-FTIR spectra of MX-PVA after 0 days (*a*), 60 days (*b*) and 120 days (*c*) of composting

C=O groups in the MX-PVA after 60 days composting. This also confirms the formation of β-hydroxylketone and 1, 3-diketone groups by a random cleavage of the polymer chains as shown by others [9, 37, 38]. In the ATR-FTIR spectrum (c), a sharper absorption observed at 1,750–1,600 cm^{-1} indicates presence of much more C=O groups in the MX-PVA after 120 days of composting. This indicates that with composting time as degradation proceeds, more ketone groups are generated. In summary, the MX-PVA specimens also degrade during composting but the change is not as significant as pure PVA or GX-PVA, due to higher crosslinking.

The effects of composting time on the MFC-PVA and HNT-PVA nanocomposites were identical to pure with PVA based on ATR-FTIR spectra where only PVA degraded leaving MFC and HNT intact, within the 120 days of composting.

DSC Study

The melting temperatures (T_m), enthalpies (ΔH_f) of fusion and crystallinity values observed in DSC scans for control and crosslinked PVA based resins and nanocomposites as a function of composting time are presented in Table 1. It is interesting to note that both T_m and ΔH_f for all specimens, including PVA, GX-PVA, MX-PVA, MFC-PVA and HNT-PVA nanocomposite specimens increased with composting time during the initial 45 days. The crystallinity values for all the specimens were calculated based on 138.6 J/g for 100 % crystalline PVA [61–64]. After 45 days of composting, T_m and crystallinity increased from 196.1 °C and 44.8 % to 210.1 °C and 53.6 %, respectively, for PVA, from 175.6 °C and 39.9 % to 200.8 °C and 49.5 % for GX-PVA, from 188.2 °C and 33.8 % to 193 °C and 50.0 % for MX-PVA, from 198.6 °C and 37.2 % to 208.3 °C and 50.4 % for MFC-PVA nanocomposites and from 199.7 °C and 40.0 to 210.1 °C and 47.6 % for HNT-PVA nanocomposites. This increase of crystallinity is a result of two main factors. The first factor, as mentioned earlier, is that the microbes (fungi) attack the amorphous domain first and digest it away. As the amorphous fraction decreases, the percent crystallinity in the remaining resin increases [3]. Similarly, hydrolytic degradation also occurs primarily in the amorphous region contributing to increase in crystallinity [2, 3, 65, 66]. Similar increase in crystallinity was observed for polyester fibers and soy protein isolate films earlier [2, 3, 62, 63]. The second factor is that the oligomeric PVA species in the amorphous regions acquire more chain mobility during composting, because of the absorbed moisture enabling them get incorporated into the existing crystals [65–67]. This process, involving an increase in the density due to higher crystallinity, is called

Table 1 Effect of composting time on the melting temperature and melting enthalpy of PVA based resins and nanocomposites

Composting time (days)/properties	PVA	GX-PVA	MX-PVA	MFC-PVA nanocomposite (10 % MFC)	HNT-PVA nanocomposite (10 % HNTs)
0/T_m (°C)	196.1	175.6	188.2	198.6	199.7
Enthalpy (J/g)	62.1	55.3	46.9	51.6	55.4
Crystallinity (%)	44.8	39.9	33.8	37.2	40.0
30/T_m (°C)	206.9	199.2	192.4	204.8	208.2
Enthalpy (J/g)	68.6	64.6	47.9	58.1	61.2
Crystallinity (%)	49.5	46.6	34.6	41.9	44.3
45/T_m (°C)	210.1	200.8	193.0	208.3	210.1
Enthalpy (J/g)	74.3	68.6	50.0	69.8	66.0
Crystallinity (%)	53.6	49.5	36.1	50.4	47.6
60/T_m (°C)	210.8	199.2	192.7	209.9	211.7
Enthalpy (J/g)	76.6	70.3	50.1	70.0	66.5
Crystallinity (%)	55.3	50.7	36.1	50.5	48.0
75/T_m (°C)	210.6	202.4	193.1	210.6	211.4
Enthalpy (J/g)	76.8	69.7	50.4	68.4	65.6
Crystallinity (%)	55.4	50.3	36.4	49.4	47.3
90/T_m (°C)	212.5	205.9	194.0	211.5	213.0
Enthalpy (J/g)	81.0	74.1	54.7	72.0	69.8
Crystallinity (%)	58.4	53.5	39.0	51.9	50.4
120/T_m (°C)	211.8	205.3	195.0	211.0	212.6
Enthalpy (J/g)	81.4	72.8	54.3	71.1	69.4
Crystallinity (%)	58.7	52.5	39.2	51.3	50.1

chemicrystallization [65–67]. This process also increases T_m and ΔH_f values as seen by others [65–67]. Changes in T_m and ΔH_f values for all the specimens were less significant between 45 and 75 days of composting. However, they increased quickly between the 75 and 90 days of composting. This indicates that more amorphous PVA biodegraded and was incorporated into existing crystals during this period. This was confirmed from the SEM and weight loss observations. However, both T_m and ΔH_f for all the specimens remained constant or even slightly decreased between the 90 and 120 days of composting, even though all specimens degraded significantly. It is very likely that both enzymes and moisture started affecting both crystalline and amorphous regions simultaneously [68].

Based on the results presented in Table 1 and results obtained in our previous research, following conclusions may be made [6, 7]. After glyoxal and MA crosslinking, the T_m, ΔH_f and crystallinity values decreased. Lower ΔH_f and crystallinity values after crosslinking are quite common as the crosslinked polymers cannot crystallize. This phenomenon has been observed in most polymers [6, 7, 57, 69–71]. The T_m for the MFC-PVA nanocomposite (198.6 °C) was close to that obtained for PVA. No T_m for cellulose can be observed as it degrades prior to melting [72, 73]. As a result, the DSC thermogram mainly represented the PVA behavior. The ΔH_f and the crystallinity of the PVA in MFC-PVA nanocomposites were 51.6 J/g and 37.2 %, respectively, which were much lower than 62.1 J/g and 44.8 %, respectively, obtained for control PVA. It is likely that the well dispersed nano- and micro-fibrils in the MFC can inhibit the crystallization of PVA. The fibrils can suppress polymeric chain movement restricting their ability to fold and thus lower the crystallinity [74]. The T_m for the HNT-PVA nanocomposite (199.7 °C) was 3.6 °C higher than that of control PVA. This suggests that HNTs have the ability to lead to slightly increased T_m of polymers [75]. The ΔH_f (55.4 J/g) and the crystallinity (40 %) of the PVA in HNT-PVA nanocomposite (10 % loading), however, were much lower than 62.1 J/g and 44.8 %, respectively, obtained for control PVA.

Sol–Gel Analysis

The gel percentages for PVA, GX-PVA and MX-PVA specimens as a function of composting times are presented in Table 2. As seen in Table 2, the gel percentage before and during composting was 0 %, for the control PVA specimens. However, in the case of crosslinked GX-PVA, the gel percentage increased from 7.0 to 7.5 % after 30 days of composting. This initial increase in gel percentage is due to the preferential leaching out of the non-crosslinked part during the first 30 days of composting. Thereafter, gel percentages of the specimen decreased and reached 4.6 and 4.4 % after 90 and 120 days of composting respectively. This indicates that composting process can break crosslinks and reduce the gel percentage, although, the process seems to be slow. In the case of MX-PVA the reduction in gel percentage was similar. After 30 days of composting, the gel percentage remained unchanged. Thereafter, gel percentages of the specimen decreased only slightly to 87.9 % after 120 days of composting. Slow cleavage/breakage of crosslinks and hence slower degradation may be used advantageously to increase the life of the resin or the nanocomposite.

Table 2 Effect of composting time on the gel (%) of PVA, GX-PVA and MX-PVA

Composting time (days)	PVA	GX-PVA	MX-PVA
0	0	7.0	90.3
30	0	7.5	90.5
45	0	4.9	89.1
60	0	4.9	88.6
75	0	5.0	88.5
90	0	4.6	88.5
120	0	4.4	87.9

Conclusions

In this study the biodegradation of PVA based materials, crosslinked, non-crosslinked and nanocomposites, in a composting medium was characterized. Chicken dropping-based compost medium was used. Composting study was carried out for up to 120 days and biodegradation was characterized using several techniques. The results suggest that biodegradation of PVA based materials in compost medium is mainly by fungal means. The enzymes secreted by fungi degrade amorphous regions of the specimens first and crystallinity plays an important role in lowering PVA biodegradation rate. The surface roughness of the specimens increased with composting time which could facilitate microorganism to stay and propagate, accelerating the degradation. Being in the form of thin sheets all specimens broke up into smaller pieces after 120 days of composting. The results also showed that crosslinking and addition of specific fillers such as high crystalline MFC and nanoclay HNTs can decrease the biodegradation rate. These results suggest that crystallinity, crosslinking and addition of suitable fillers may be used to control the service life of the PVA based biodegradable nanocomposites.

Acknowledgments This work was partly supported by the National Textile Center (NTC), the Wallace Foundation and the Department of Fiber Science & Apparel Design at Cornell University. The authors also thank the Cornell Center for Materials Research (CCMR) for the

use of their facilities and Cornell Poultry Research Farm for providing compost material.

References

1. Cho D, Netravali AN, Joo YL (2012) Mechanical properties and biodegradability of electronspun soy protein isolate/PVA hybrid nanofibers. Polym Degrad Stab 97:747–954
2. Luo S, Netravali AN (2003) A study of physical and mechanical properties of poly(hydroxybutyrate-co-hydroxyvalerate) during composting. Polym Degrad Stab 80:59–66
3. Lodha P, Netravali AN (2005) Effect of soy protein isolate resin modifications on their biodegradation in a compost medium. Polym Degrad Stab 87:465–477
4. Qiu K, Netravali AN (2012) Biodegradable composites of polyvinyl alcohol reinforced with microfibrillated cellulose. J Mater Sci 47(16):6066–6075
5. Qiu K, Netravali AN (2013) 'Green' composites based on bacterial cellulose produced using novel low cost carbon source and soy protein resin. Recent advances in adhesion science & technology: Mittal festschrift. Taylor & Francis, London (in press)
6. Qiu K, Netravali AN (2012) Fabrication and characterization of biodegradable composites based on microfibrillated cellulose and polyvinyl alcohol. Compos Sci Technol 72(13):1588–1594
7. Qiu K, Netravali AN (2013) Halloysite nanotube reinforced biodegradable nanocomposites using noncrosslinked and malonic acid crosslinked polyvinyl alcohol. Polym Compos. doi:10.1002/pc.22482
8. Stevens ES (2002) Green plastics: an introduction to the new science of biodegradable plastics. Princeton University Press, Princeton, pp 10–30
9. Chiellini E, Corti A, D'Antone S, Solaro R (2003) Biodegradation of poly (vinyl alcohol) based materials. Prog Polym Sci 28:963–1014
10. Netravali AN, Chabba S (2003) Composites get greener. Mater Today 6(4):22–29
11. Georgia Tech Research Institute (2011) 'Breaking down plastics: new standard specification may facilitate use of additives that trigger biodegradation of oil-based plastics in landfills'. http://gtresearchnews.gatech.edu/biodegradation-of-plastics/
12. Mittal V (2011) Nanocomposites with biodegradable polymers: synthesis, properties and future perspectives. Oxford University Press, Oxford, pp 1–27
13. Bohlmann GM (2005) General characteristics, processability, industrial applications and market evolution of biodegradable polymers. In: Bastioli C (ed) Handbook of biodegradable polymers. Rapra Tech Ltd, Shawbury, pp 183–218
14. Lemm W, Krukenberg T, Regier G, Gerlach K, Bucherl ES (1981) Biodegrdation of some biomaterials after subcutaneous implantation. Proc Eur Sco Artif Org 8:71–75
15. Potts JE, Clendinning RA, Ackart WB, Neigisch WD (1973) The biodegradability of synthetic polymers. In: Guillet J (ed) Polymers and ecological problems. Plenum Press, New York, pp 61–80
16. Swift G (1992) Biodegrdable polymers in the environment: are they really biodegradable? Pro ACS Div Polym Mater Sci Eng 66:403–404
17. Ratner BC, Gladhill KW, Horbett TA (1988) Analysis of in vitro enzymatic and oxidative degradation of polyurethane. J Biome Mater Res 22:509–527
18. Hergenrother RW, Wabers HD, Cooper SL (1992) The effect of chain extenders and stabilizers on the in vivo stability of polyurethanes. J Appl Biomater 3:17–22
19. Reich L, Stivala SS (1971) Elements of polymer degradation. McGraw-Hill, New York
20. Kronenthal RL (1975) Biodegradable polymers in medicine and surgery. In: Kronenthal RL, Oser Z, Martin E (eds) Polymers in medicine and surgery. Plenum Press, New York, pp 119–133
21. Gilding DK (1981) Biodegradable polymers. In: Williams DF (ed) Biocompatibility of clinic implant materials. CRC Press, Boca Raton, pp 209–232
22. Itavaara M, Karjomaa S, Selin JF (2002) Biodegradation of polyolactide in aerobic and anaerobic thermophilic conditions. Chemosphere 46:879–885
23. Tokiwa Y, Suzuki T (1978) Hydrolysis of polyesters by rhizopus delemar lipase. Agric Biol Chem 42:1071–1072
24. Tokiwa Y, Suzuki T (1981) Hydrolysis of copolyesters containing aromatic and aliphatic ester blocks by lipase. J Appl Polym Sci 26:441–448
25. Tokiwa Y, Suzuki T, Ando T (1979) Synthesis of copolyamide-esters and some aspects involved in their hydrolysis by lipase. J Appl Polym Sci 24:1701–1711
26. Tokiwa Y, Calabia BP, Ugwu CU, Aiba S (2009) Biodegradability of plastics. Int J Mol Sci 10:3722–3742
27. Corti A, Solaro R, Chiellini E (2002) Biodegradation of poly (vinyl alcohol) in selected mixed microbial culture and relevant culture filtrate. Polym Degrad Stab 75(3):447–458
28. Lodha P (2004) Fundamental approaches to improving performance of soy protein isolate based 'green' plastics and composites. PhD Dissertation, Cornell University, Ithaca, NY, pp 101–129
29. Semenov SA, Gumargalieva KZ, Zaikov GE (2003) Biodegrdation and durability of materials under the effect of microorganisms. VSP BV, Boston
30. Han SI, Lim JS, Kim DK, Kim MN, Im SS (2008) In situ polymerized poly (butylene succinate)/silica nanocomposites: physical properties and biodegradation. Polym Degrad Stab 93:889–895
31. Yang HS, Yoon JS, Kim MN (2005) Dependence of biodegradability of plastics in compost on the shape of specimens. Polym Degrad Stab 87:131–135
32. Ray SS, Okamoto M (2003) Biodegradable polylactide and its nanocomposites; opening a new dimension for plastics and composites. Macromol Rap Comm 24:815–840
33. Fukuda N, Tsuji H, Ohnishi Y (2002) Physical properties and enzymatic hydrolysis of poly (-latide)-$CaCO_3$ composites. Polym Degrad Stab 78:119–127
34. Quynh TM, Mitomo H, Nagasawa N, Wada Y, Yoshii F, Tamada M (2007) Properties of crosslinked polylactides (PLLA & PDLA) by radiation and its biodegradability. Euro Polym J 43:1779–1785
35. Solaro R, Corti A, Chiellini E (2000) Biodegradation of poly (vinyl alcohol) with different molecular weight and degree of hydrolysis. Polym Adv Technol 11(8–12):873–878
36. Vijayalakshmi SP, Madras G (2006) Effects of the pH, concentration, and solvents on the ultrasonic degradation of poly(vinyl alcohol). J Appl Polym Sci 100(6):4888–4892
37. Watanabe Y, Morita M, Hamada N, Tsujisaka Y (1975) Formation of hydrogen peroxide by a polyvinyl alcohol degrading enzyme. Agric Biol Chem 39:2447–2448
38. Suzuki T, Ichihara Y, Yamada M, Tonomura K (1973) Some characteristics of *Pesudomonas* O-3 which utilize polyvinyl alcohol. Agric Biol Chem 37:747–756
39. Sakai K, Hamada N, Watanabe Y (1986) Studies on the poly(-vinyl alcohol)-degrading enzyme. Part VI. Degradation mechanism of poly(vinyl alcohol) by successive reactions of secondary alcohol oxidase and β-diketone hydrolase from *Pseudomonas* sp. Agric Biol Chem 50:989–996

40. Jecu L, Grosu E, Raut I, Ghiurea M, Constantin M, Stoica A, Stroescu M, Vasilescu G (2012) Fungal degradation of polymeric materials: morphological aspects. http://www.inginerie-electrica.ro/acqu/2011/P_1_Fungal_degradation_of_polymeric_materials_Morfological_aspects.pdf
41. Larking DM, Crawford RJ, Christie GBY, Lonergan GT (1999) Enhanced degradation of polyvinyl alcohol by *Pysnoporus cinnabarinus* after pretreatment with Fenton's reagent. Appl Environ Microbiol 65(4):1798–1800
42. Chiellini E, Corti A, Solaro R (1999) Biodegradation of poly (vinyl alcohol) based blown films under different environmental conditions. Polym Degrad Stab 64:305–312
43. Jayasekara R, Harding I, Bowater I, Christie GBY, Lonergan GT (2003) Biodegradation by composting of surface modified starch and PVA blended films. J Polym Environ 11(2):49–56
44. Solaro R, Corti A, Chiellini E (1998) A new respirometric test simulating soil burial conditions for the evaluation of polymer biodegradation. J Environ Polym Degrad 6:203–208
45. Matsumura S, Tanaka T (1994) Novel malonate-type copolymers containing vinyl alcohol blocks as biodegradable segments and their builder performance in detergent formulation. J Environ Polym Degrad 2:89–97
46. Diaz LF, Savage GM, Eggerth LI, Golueke CG (1993) Composting and recycling-municipal solid waste. Lewis Publishers, Boca Raton
47. Maiti S, Ray D, Mitra D (2012) Role of crosslinker on the biodegradation behavior of starch/polyvinylalcohol blend films. J Polym Environ 20:749–759
48. Chai W, Chou J, Chen C (2012) Effects of modified starch and different molecular weight polyvinyl alcohols on biodegradable characteristics of polyvinyl alcohol/starch blends. J Polym Environ 20:550–564
49. Jian S, Ming SX (1987) Crosslinked PVA-PS thin-film composite membrane for reverse osmosis. Desalination 62:395–403
50. Majumdar S, Adhikari B (2006) Polyvinyl alcohol: a taste sensing material. Sensors Actuators B-Chem 114:747–755
51. Huang X, Netravali AN (2008) Environmentally friendly green materials from plant-based resources: modification of soy protein using Gellan and micro/nano-fibrillated cellulose. J Macromol Sci A 45:899–906
52. Rathi P (2007) Soy protein based nanophase reins for green composites. A project report, Cornell University, Ithaca, NY, pp 13–18
53. Rudnik E (2008) Compostable polymer materials. Elsevier, Oxford, pp 89–112
54. Sang BI, Hori K, Tanji Y, Unno H (2002) Fungal contribution to in situ biodegradation of poly (3-hydroxybutyrate-co-3-hydroxyvalerate) film in soil. Appl Microbiol Biotechnol 58:241–247
55. Taixing Shenlong Chemical Co., Ltd (2012) Crystal ortho phosphorous acid. http://www.sl-chemical.com/pages/pro4_en.htm
56. Jeffries Group (2011) Compost creating cool cucumbers. http://www.jeffries.com.au/about-us/news/article/cucumbers
57. BASF (2011) Glyoxal-the sustainable solution for your business. http://worldaccount.basf.com/wa/NAFTA/Catalog/ChemicalsNAFTA/doc4/BASF/PRD/30037091/.pdf?title=Brochure&asset_type=pi/pdf&language=EN&urn=urn:documentum:eCommerce_sol_EU:09007bb2800475c8.pdf
58. Gohil JM, Bhattacharya A, Ray P (2006) Studies on the cross-linking of poly (vinyl alcohol). J Polym Res 13:161–169
59. Mansur HS, Sadahira CM, Souza AN, Mansur AAP (2008) FTIR spectroscopy characterization of poly (vinyl alcohol) hydrogel with different hydrolysis degree and chemically crosslinked with glutaraldehyde. Mater Sci Eng C 28:539–548
60. Kim JH, Moon EJ, Kim CK (2003) Composite membranes prepared from poly (m-animostyrene-co-vinyl alcohol) copolymers for the reverse osmosis process. J Membr Sci 216:107–120
61. Warner SB (1995) Fiber science. Prentice Hall, Upper Saddle River, pp 205–206
62. Blaine RL (2011) Determination of polymer crystallinity by DSC. TA Instruments, www.tainstruments.com/library_download.aspx?file=TA123.PDF
63. Sichina WJ (2011) DSC as problem solving tool: measurement of percent crystallinity of thermoplastics. PerkinElmer Instruments. http://www.perkinelmer.com/Content/applicationnotes/app_thermalcrystallinitythermoplastics.pdf
64. Guirguis OW, Moselhey MTH (2012) Thermal and structural studies of poly (vinyl alcohol) and hydroxypropyl cellulose blends. Nat Sci 4(1):57–67
65. Netravali AN, Krstic R, Crouse JL, Richmond LE (1993) Chemical stability of polyester fibers and geotextiles without and under stress. ASTM, STP 1190:207–217
66. Mathur A, Netravali AN, O'Rourke D (1994) Chemical aging effects on the physic-mechanical properties on the polyester and polypropylene geotextiles. Geotext Geomembr 13:591–626
67. Jailloux JM, Verdu J (1990) Kinetic models for the life prediction in PET hygrothermal aging: a critical survey. In: Hoedt D (ed) Proceedings of 4th international conference on geotextiles, geomembranes and related products. Balkema, Rotterdam, p 727
68. Bikiaris DN, Papageorgious GZ, Achili DS (2006) Synthesis and comparative biodegradability studies of three (alkylene succinate)s. Polym Degrad Stab 91(1):31–43
69. Young RJ, Lovell PA (2011) Introduction to polymers, 3rd edn. CRC Press, Boca Raton, pp 591–622
70. Kim JH, Kim JY, Lee YM, Kim KY (1992) Properties and swelling characteristics of cross-linked poly (vinyl alcohol)/chitosan blend membrane. J Appl Polym Sci 45(10):1711–1717
71. Mtshali TN, Krupa I, Luyt AS (2001) The effect of cross-linking on the thermal properties of LDPE/wax blends. Thermalchim Acta 380:47–54
72. Gardner DJ, Oporto GS, Mills R, Samir MASA (2008) Adhesion and surface issues in cellulose and nanocellulose. J Adhes Sci Technol 22:545–567
73. Yan C, Zhang J, Lv Y, Yu J, Wu J, Zhang J, He J (2009) Thermoplastic cellulose-graft-poly (L-lactide) copolymers homogeneously synthesized in an ionic liquid with 4-deimethylaminopyridine catalyst. Biomacromolecules 10(8):2013–2018
74. Boudenne A, Ibos L, Candau Y, Thomas S (2011) Handbook of multiphase polymer systems. Wiley, Chichester, p 455
75. Liu M, Guo B, Du M, Chen F, Jia D (2009) Halloysite nanotubes as a novel β-nucleating agent for isotactic polypropylene. Polymer 50:3022–3030